



Renoprotective effects of *Strychnos potatorum* seed extract in streptozotocin-induced diabetic nephropathy: Enhancement of antioxidant defenses and Zonula occludens – 1 expression

Abarajitha Shankaranarayanan^{1,2}, Manickam Subramanian^{3*}, Sharmila Aristotle¹, Sundarapandian Subramanian², Prabhu Kaliyaperumal⁴

¹Department of Anatomy, Chettinad Hospital and Research Institute, Chettinad Academy of Research and Education, Kelambakkam, India.

²Department of Anatomy, SRM Medical College Hospital and Research Centre, Faculty of Medicine and Health Sciences, SRM Institute of Science and Technology, Kattankulathur, India.

³Department of Anatomy, PSP Medical College Hospital and Research Institute, Chennai, India.

⁴Department of Anatomy, Sree Balaji Medical College, Bharath Institute of Higher Education and Research, Chennai, India.

ARTICLE HISTORY

Received on: 10/12/2025
Accepted on: 04/03/2026
Available Online: 15/04/2026

Key words:

Strychnos potatorum, Zonula occludens – 1, Oxidative stress, Streptozotocin, Glomerular filtration barrier.

ABSTRACT

Diabetic nephropathy (DN), a severe microvascular complication of diabetes mellitus, is a leading cause of end-stage renal disease. Current therapies that focus on glycemic and blood pressure control are insufficient, prompting the need for novel interventions. While the systemic metabolic effects of ethanolic extract of *Strychnos potatorum* seeds (EESP), including changes in body weight, blood glucose, and insulin levels, and its role in upregulation of fibroblast-specific protein-1, have been previously reported, this study investigated the renoprotective potential of the EESP in a streptozotocin-induced rat model of DN. The study focused on the modulation of the tight junction protein Zonula occludens – 1 (ZO-1), which maintains the integrity of the glomerular filtration barrier. Thirty male Wistar albino rats were divided into five groups and treated with EESP (500 mg/kg) or metformin (50 mg/kg) for 30 days. Urine analysis, renal histopathology, electron microscopy study, ZO-1 immunohistochemistry, gene expression, and protein expression were analyzed. EESP administration significantly improved renal function by reducing the urinary albumin ($p = 0.03$), protein ($p = 0.01$), urea, and creatinine levels. It alleviated oxidative stress markers such as lipid peroxidation, hydrogen peroxide, and protein carbonyls, while restoring antioxidant enzyme (glutathione peroxidase, glutathione S-transferase, superoxide dismutase, and catalase) activity ($p = 0.001$). Histological and ultrastructural analyses revealed reduced glomerular basement membrane thickening, tubular atrophy, and podocyte damage. Notably, EESP upregulated ZO-1 expression at both the gene (2.25-fold) and protein (3.6-fold) levels, suggesting improved slit diaphragm integrity and reduced proteinuria. These findings suggest that EESP offers a multifaceted renoprotective effect in DN through the mitigation of oxidative stress, structural preservation, and enhancement of ZO-1 expression. Further mechanistic and clinical studies are warranted to validate *S. potatorum* as a potential therapeutic candidate for DN.

1. INTRODUCTION

Chronic hyperglycemia in individuals with diabetes mellitus (DM) predisposes them to a range of complications

that substantially contribute to higher morbidity and mortality rates [1]. Diabetic nephropathy (DN) is the most severe complication associated with DM. It affects nearly one-third of diabetic patients and represents a major clinical concern owing to its progressive nature and poor prognosis if left untreated [2]. Between 1990 and 2021, DN-related mortality increased substantially from 197.27 to 571.29 million cases [3]. In India, the epidemiology of DN is particularly concerning, given the country's large and rapidly expanding diabetic population. The prevalence of DN in India varies widely, from 0.9% to as high as

*Corresponding Author
Manickam Subramanian, Department of Anatomy, PSP Medical College Hospital and Research Institute, Chennai, India.
E-mail: gandhiayu@hotmail.com

62.3%, reflecting regional differences and study methodologies [4]. DN is clinically characterized by albuminuria with urinary albumin excretion rates exceeding 300 mg/day, diminished glomerular filtration rate (GFR), and progressive decline in renal function [5]. This condition has become the primary cause of end-stage renal disease (ESRD), which is associated with permanent renal damage and necessitates intensive therapeutic intervention [5]. The pathological changes in ESRD include glomerular hyperfiltration, increased albuminuria, microalbuminuria, and progressive proteinuria. The incidence of ESRD continues to rise with an increase in prevalence of DN and leading to a growing demand for dialysis and kidney transplantation to support life and mitigate disease-associated morbidity [6].

The slit diaphragm (SD) is a highly specialized zipper-like structural component critical for maintaining the selective permeability of the glomerular filtration barrier [7]. In DN, the early preservation of SD integrity through therapeutic intervention is crucial for mitigating disease progression. Similarly, tight junctions (TJ) represent another essential cellular structure formed by direct membrane-to-membrane contact, particularly within podocytes of the glomeruli. TJ plays a fundamental role in mediating intercellular communication and regulating signaling pathways [8]. Podocyte-specific TJs are primarily made of proteins like junctional adhesion molecule A, occludin, and Zonula occludens – 1 (ZO-1), all of which are essential for controlling the passage of water, solutes, and proteins across the glomerular barrier [8,9]. Under pathological nephrotic conditions, disruption of the SD structure often results in its transition toward a TJ configuration, known as the SD-TJ transition [10]. This pathological transition is frequently associated with the effacement of podocyte foot processes [11]. Evidence suggests that inhibition of SD-TJ transition has a protective effect, helping stabilize the SD structure and reduce proteinuria in nephrotic conditions, including DN [12]. While nephrin and podocin are crucial components of the SD, and claudin-1 is implicated in its destabilization, we chose to focus on ZO-1 due to its multifaceted role as a key scaffold protein that interconnects SD components with the actin cytoskeleton, and critically, its direct involvement in the pathological SD-TJ transition observed in DN. Therefore, ZO-1 is instrumental in inhibiting epithelial-mesenchymal transition (EMT) and supporting the restoration of the SD [13]. By targeting ZO-1, we aimed to investigate a protein that not only reflects the integrity of the glomerular barrier but also plays an important role in dynamic pathological changes that lead to its dysfunction in DN.

Despite advances in our understanding of DN, current therapeutic approaches, which focus primarily on glycemic and blood pressure control, are often insufficient to halt disease progression towards ESRD and reduce DN-related mortality. Pharmacological interventions such as oral hypoglycemic drugs and insulin are widely used, with dosing adjusted according to the patient's glomerular GFR and renal function [14]. However, these treatments primarily delay disease progression rather than offering a curative solution. Consequently, there is a growing need for novel therapeutic agents that target the multifaceted mechanisms underlying DN, such as oxidative stress and structural integrity of the glomerular filtration barrier [15].

Given the complex pathophysiology of DN, traditional medicinal plants, such as *Strychnos potatorum*, belonging to the Loganiaceae family, may offer promising therapeutic insights. Powder and water extracts of *S. potatorum* seeds are used to treat disorders such as urinary strangulation, urinary incontinence, gonorrhoea, and liver and kidney ailments in Ayurveda and Unani systems of medicine [16]. A previous study by our research group revealed a rich profile of secondary metabolites present in the ethanolic seed extract of *Strychnos potatorum* (EESP), including terpenoids, alkaloids, flavonoids, phenols, tannins, and saponins. High performance thin layer chromatography analysis confirmed that terpenoids were the most abundant class of compounds. Gas chromatography – mass spectrometry analysis identified 17 bioactive compounds, such as imidazole, 9,12-octadecadienoic acid, 1-butanone 1-(2-hydroxyphenyl), imidazole 2-fluoro-1-triacetylribofuranosyl, and flavone with promising pharmacological potential, including antioxidant, anti-inflammatory, antibacterial, and antitumor properties. Bioinformatics evaluation showed that the majority of these compounds adhered to Lipinski's rule of five, indicating good drug-like properties and oral bioavailability. The EESP exhibited significant *in vitro* antioxidant activity, comparable to that of ascorbic acid, suggesting its potential therapeutic use in treating oxidative stress-related disorders, including cancer and diabetes [17]. Toxicological studies using Wistar albino mice and rats have demonstrated the safety of *S. potatorum* extracts at a dosage up to 2,000 mg/kg. Notably, no toxic effects were observed even during 90-day chronic exposure trials at dosages ranging from 100 to 200 mg/kg [18].

Given the multifaceted nature of DN, our previous work has thoroughly investigated the systemic metabolic effects of *S. potatorum* seed extract, including its impact on body weight, blood glucose, insulin, serum creatinine, and urea levels in a similar diabetic rat model. In addition, we have reported the role of *S. potatorum* seed extract in downregulating the renal expression of fibroblast-specific protein-1 (FSP-1), a key protein involved in renal fibrosis through EMT [19].

While the general nephroprotective and antidiabetic properties of *S. potatorum* have been documented [20,21], its specific mechanism involved in ameliorating DN through the modulation of tight junction proteins, especially ZO-1, remains unexplored. The present study directly addresses this critical gap by investigating whether the EESP can exert nephroprotective effects in streptozotocin (STZ)-induced DN by enhancing renal antioxidant status and crucially, by modulating ZO-1 expression to maintain glomerular barrier integrity. Therefore, this study extends our prior work on FSP-1 [19] by focusing on ZO-1-mediated barrier integrity.

2. MATERIALS AND METHODS

2.1. Authentication of plant material and preparation of extract

Seeds of *S. potatorum* were obtained from a local marketplace and subsequently verified and authenticated by the Siddha Central Research Institute (Arumbakkam) under reference number 339.18082201, dated 18/08/2022. Coarsely powdered and desiccated *S. potatorum* seeds were immersed

in 95% ethanol (1:10 w/v, sample to solvent) for 48 hours. The resulting filtrate was then introduced into the thimble of a Soxhlet extraction apparatus, with four extraction cycles conducted per hour over a 12-hour period at a temperature of 70°C. To ensure consistent and reliable results, the extraction was replicated across three independent batches under identical conditions. Following the extraction process, the resultant extract was stored in an airtight container to yield 25% w/w.

2.2. Experimental animals

The experiment was initiated after obtaining permission from the Institutional Animal Ethics Committee (1/ Proposal:105/A. Lr: 78, Dt: 13.02.2023) following the guidelines framed by the Committee for the Purpose of Control and Supervision of Experiments on Animals. Being an exploratory study with ethical limits, thirty adult Wistar albino male rats (weighing ~250 g) were randomly allocated into five groups ($n = 6$ per group) using a randomization schedule generated by a web-based Research Randomizer tool (www.randomizer.org). Each animal was assigned a unique identification number, which was used for random group allocation. The allocation sequence was generated and maintained by an independent researcher who was not involved in animal handling, treatment administration, or data collection. The study is assumed to have a medium effect size ($f = 0.25$), and reduction in urinary urea, creatinine, albumin, and glomerular basement membrane (GBM) thickening were the primary outcomes. The animals were sheltered in an institutional animal facility under standard conditions and allocated equally into five groups as given below. The animals were given a standard commercial pellet diet (VRK Nutritional Laboratory Rat Mice Pellets, Pune, India) and distilled water ad libitum.

Group I: Control

Group II: EESP

Group III: DN

Group IV: DN + EESP, and

Group V: DN +Metformin (MET).

2.3. Induction of diabetes

The induction of STZ-induced diabetes was performed following the methodology outlined by Punithavathi *et al.* [22]. Prior to the induction of diabetes, baseline fasting blood sugar levels were assessed to verify the non-diabetic status of the animals. Rats from groups III–V received a single intraperitoneal injection of STZ (50 mg/kg, SRL Pvt. Ltd., India, # 14653), which was prepared in a cold citrate buffer (0.1M, pH 4.5). To mitigate mortality due to hypoglycemia, diabetic rats were administered a 20% glucose solution. After 3 days, rats exhibiting fasting blood sugar levels ≥ 250 mg/dl were included in the study. Detailed systemic metabolic parameters, including body weight changes and blood glucose, insulin, urea, and creatinine levels throughout the study period, have been previously reported by our group [19].

2.4. Administration of experimental drugs

Animals in Groups II and IV were administered 500 mg/kg body weight of EESP, while those in Group V received 50 mg/kg body weight of MET (Sigma-Aldrich USA,

PHR1084) orally for a duration of 30 days. The experimental drugs were prepared and coded by an independent researcher who was not involved in animal handling, treatment, or data collection. The investigator responsible for administering the treatments was blinded to the group allocation throughout the study.

2.5. Sample collection

Throughout the experiment, the food and water levels were monitored daily, and urine samples were obtained from the rats using metabolic cages 2 days before the end of the study and subsequently preserved for the assessment of albumin, protein, urea, and creatinine levels in the urine. Upon conclusion of the study, the animals were euthanized using halothane, and the kidneys were collected. One set of kidneys was used for histopathological examination and electron microscopy (EM) studies and preserved in formaldehyde (10%) and glutaraldehyde, respectively. The other set of kidneys was designated for western blotting and gene expression analyses. Samples were coded prior to analysis, and the codes were broken after all analyses were completed and a preliminary interpretation of the results.

2.6. Urine analysis

Twenty-four-hour urine samples were collected using metabolic cages. Debris from the samples was removed by centrifugation at 3,000 rpm for 10 minutes. The concentrations of urea (urease method, #E-BC-K183-S), creatinine (Sarcosine oxidase method, #E-BC-K188-M), albumin (Bromocresol Green method, #E-BC-K057-M), and total protein (# E-BC-K252-M) in the urine were assessed using commercial colorimetric assay kits (Elabscience, TX), adhering to the instructions provided by the manufacturer.

2.7. Kidney antioxidant assays

Kidney tissue samples were homogenized in Tris-HCl buffer and centrifuged (3,000 \times , 10 minutes, 4°C). Enzymatic and nonenzymatic antioxidant analyses were conducted using the supernatant. The levels of thiobarbituric acid-reactive substances were quantified spectrophotometrically (532 nm) to assess lipid peroxidation (LPO), following the methodology outlined by Jittiwat *et al.* [23]. The levels of glutathione peroxidase (GPx), glutathione S-transferase (GST), superoxide dismutase (SOD), and protein carbonyl (PC) were analyzed spectrophotometrically according to the procedures outlined by Farhat *et al.* [24] (412 nm), Varadacharyulu *et al.* [25] (340 nm), Atamanalp *et al.* [26] (480 nm), and Zahouani *et al.* [27] (370 nm). The catalase (CAT) activity was assessed (620 nm) using the method adopted by Payamalle *et al.* [28]. Hydrogen peroxide activity was quantified by dichlorodihydrofluorescein diacetate staining (using a fluorescence microplate reader with 488 and 530 nm as excitation and emission wavelengths, respectively).

2.8. Histopathology

Four-micron-thick paraffin sections were prepared from formalin-fixed renal specimens and were subsequently stained with hematoxylin and eosin (H&E) and Periodic acid-

Schiff (PAS) to examine pathological changes and thickening of the GBM.

2.9. EM study

From each group, one representative kidney sample was selected from one animal and fixed with glutaraldehyde. These tissues were then processed and encapsulated within siliconized rubber moulds using an epoxy resin. Ultrathin sections were transferred onto copper grids and stained with uranyl acetate and the Reynolds solution. The sections were observed under a Philips TecnaiT12 Spirit transmission electron microscope, and images were captured.

2.10. Immunohistochemistry (IHC)

Renal tissue sections, measuring 8 μm in thickness, underwent antigen retrieval through the application of a citrate buffer (0.01 mol/l, pH 6.0) at a temperature of 85°C for a period of 5 minutes. The slides were subsequently incubated with goat serum (5%) for an hour at room temperature to inhibit background staining. Later, the sections were exposed to anti-ZO-1 antibody (rabbit polyclonal, Invitrogen, USA, cat#61-7300, 1:1000 dilution) overnight at 4°C. The sections were then treated with anti-rabbit IgG secondary antibody (1:2000 dilution) for 1 hour at 37°C. The sections were counterstained with Harris hematoxylin that stains nuclei deep blue, providing good contrast with brown diaminobenzidine IHC chromogen. For semi-quantitative analysis, images were captured using an Axio Lab A1 microscope (Carl Zeiss, Germany) and analyzed using ImageJ software (version 1.54). The mean pixel intensity of ZO-1 positive areas within the glomeruli and tubules was measured across 5 randomly selected non-overlapping fields per section from each animal. These intensity values were then used to calculate relative fold changes between groups.

2.11. Semi-quantitative reverse transcription polymerase chain reaction

Total RNA was extracted from kidney tissues preserved at -80°C utilizing TRIzol reagent (Invitrogen, USA). Total RNA was reverse transcribed into cDNA using SuperScript II Reverse Transcriptase followed by end-point polymerase chain reaction amplification (ABI PRISM 7000, USA) using the following primers: *Tightjunctionprotein 1* (*Tjp1*, genesymbol of ZO-1 gene) forward 5'-CGGTCCTCTGAGCCTGTAAG-3', reverse 5'-GGATCTACATGCGACGACAA-3'; *Actin beta* (*ACTB*, β -actin gene symbol) forward 5'-GCTTCTGGGTTCCGATGATA-3', reverse 5'-CCTGGCACACCATCATCTTG-3'. The amplified products were separated by agarose gel electrophoresis, and band intensities were quantified by densitometric analysis using Gel-Pro Analyzer software (version 4.0). ZO-1 mRNA expression levels were normalized to β -actin, and relative fold changes were calculated with respect to the control group.

2.12. Western blot analysis

Kidney samples (100 μg), after homogenization (RIPA buffer), were subjected to lysis, quantification, and immunoblot analysis following established protocols. Total protein concentration in cell lysates was determined using

the Lowry assay with bovine serum albumin standards, measuring absorbance at 740 nm [29]. The protein extracts (50 μg) were subjected to separation using 10% sodium dodecyl sulfate-polyacrylamide gel electrophoresis and subsequently transferred onto polyvinylidene difluoride membranes. The membranes were then blocked with 5% bovine serum albumin and incubated for 2 hours with ZO-1 (rabbit polyclonal, Invitrogen, USA, cat#61-7300) and glyceraldehyde-3-phosphate dehydrogenase (GAPDH, mouse monoclonal, Cell Signaling Technology, USA, cat# 51332) antibodies (1:1000 dilution). Following washing, the membranes were treated with a horseradish peroxidase-labeled secondary antibody for an hour at room temperature. The protein expression was detected using an enhanced chemiluminescence reagent. The band intensity was quantified through densitometric analysis using BIO-1D image software. The relative expression of ZO-1 protein was normalized to that of the internal loading control, GAPDH, for each sample.

2.13. Morphometric analysis

The diameters of the renal glomerulus and tubules were evaluated on H&E-stained slides at a magnification of 100 \times , using ocular and stage micrometers. Six fields chosen at random from 10 different sections of each animal were analyzed. A total of 60 fields were assessed per animal [30]. The parameters were determined using the following formula: Diameter (μm) = $(L + B) / 2$, where L denotes the maximum length of the glomerulus and tubule, and B stands for the maximum breadth of the glomerulus and tubule perpendicular to L .

2.14. Statistical analysis

The findings are presented as the mean \pm standard deviation (SD). Levene's test was performed to evaluate the homogeneity of variance. If the homogeneity of variance assumption is complied ($p > 0.05$), then the differences between the experimental groups were assessed using one-way analysis of variance (ANOVA) followed by the Tukey *post-hoc* test. Non-parametric Kruskal-Wallis H tests were used to compare groups for morphometric data, as the data violated the assumption of normality. Following a significant difference ($p = 0.01$) between groups, *post-hoc* pairwise comparison using Dunn's test with Bonferroni correction was carried out. All statistical analyses were conducted using SPSS software (version 29.0.2.0).

3. RESULTS

3.1. Impact on food and water intake

The effect of EESP on food and water consumption in rats with STZ-induced DN was assessed by comparing the intake levels at both the initiation and conclusion of the study. As presented in Table 1, Groups I and II exhibited no statistically significant differences in food and water intake between the start and end of the study. Group III showed a significant rise in food consumption, along with a marked increase in water consumption at the study's onset, which remained higher than the control group by the end of the study ($p = 0.001$ for both). Conversely, Group IV, which received EESP treatment, showed a significant reduction in food ($p = 0.003$) and water ($p = 0.001$)

intake at the end of the fourth week compared with the untreated group. MET-treated diabetic animals in Group V displayed a similar pattern to that of Group IV ($p = 0.001$ for both food and water). These findings suggest that STZ-induced DN leads to significant increases in both food and water consumption, whereas treatment with EESP and MET effectively mitigated these changes, indicating their potential therapeutic roles in addressing diabetes-related hyperphagia and polydipsia. There was a significant difference in food ($p = 0.02$) or water ($p = 0.04$) intake between the EESP- and MET-treated groups.

3.2. Effects on urea, creatinine, albumin, and protein in urine

Urine composition analysis revealed significant alterations among the experimental groups. In the DN group, there was a notable increase in albumin and protein excretion, indicative of proteinuria or albuminuria, which are critical markers of DN progression, compared to the control group ($p = 0.02$ and $p = 0.01$, respectively). However, treatment with EESP and MET significantly reduced these levels. The EESP-treated group exhibited albumin and protein levels, which were significantly lower than those in untreated animals ($p = 0.03$ and 0.01 , respectively), while the MET group had albumin and protein levels significantly lower than group III ($p = 0.01$ and 0.005 , respectively). Urea and creatinine levels followed a similar pattern, with significant increases in the DN group compared to controls, and notable reductions in the treatment groups. These findings suggest that both EESP and MET are effective in ameliorating the urinary markers of DN, with EESP demonstrating promising nephroprotective effects (Table 2).

Table 1. Food and water intake of animals at the beginning and end of the study.

Group	Food intake (g/rat/day)		Water intake (ml/rat/day)	
	Beginning	End	Beginning	End
I	8.36 ± 0.25	8.37 ± 0.74	4.52 ± 1.25	4.40 ± 0.62
II	8.34 ± 0.38	8.20 ± 0.29	4.64 ± 1.16	4.16 ± 0.68
III	13.38 ± 0.43*	16.34 ± 0.11*	32.73 ± 0.79*	32.97 ± 0.65*
IV	13.16 ± 0.12*	11.10 ± 0.28 [#]	32.02 ± 1.51*	9.88 ± 3.27 [#]
V	13.22 ± 0.12*	8.80 ± 0.25 ^{#S}	31.31 ± 1.91*	8.69 ± 1.72 ^{#S}

Results are expressed as the mean ± SD ($n = 6$). Superscripts indicate a significant difference between groups based on the paired *T* Test ($p \leq 0.05$). *: Compared with Group I; #: Compared with Group III; S: Compared with Group IV.

Table 2. Urea, creatinine, albumin, and protein levels in the urine.

Group	Urine urea (g/24 hours)	Urine creatinine (mg/24 hours)	Urine albumin (mg/24 hours)	Urine protein (mg/dl)	Urine volume (ml)
I	15.71 ± 0.17	15.78 ± 0.14	3.00 ± 0.16	1.11 ± 0.16	7.03 ± 0.22
II	15.88 ± 0.23	16.08 ± 0.16	3.13 ± 0.29	1.31 ± 0.14	6.80 ± 0.43
III	30.33 ± 0.16*	30.46 ± 0.28*	8.25 ± 0.18*	14.88 ± 0.11*	20.58 ± 1.02*
IV	19.75 ± 0.18 [#]	19.80 ± 0.14 [#]	4.66 ± 0.16 [#]	7.75 ± 0.18 [#]	9.25 ± 0.73 ^{#@}
V	18.51 ± 0.14 ^{#S}	17.78 ± 0.14 ^{#S}	3.91 ± 0.11 ^{#S}	6.35 ± 0.18 ^{#S}	10.38 ± 0.55 [#]

Results are expressed as mean ± SD ($n = 6$). Superscripts indicate a significant difference between groups based on Tukey's post hoc test following one-way ANOVA ($p \leq 0.05$). *: Compared with Group I; #: Compared with Group III; S: Compared with Group IV; @: Compared with Group V.

3.3. Effects on oxidative stress and antioxidant status

In the untreated DN group, animals exhibited significant increases in oxidative stress markers, with LPO, hydrogen peroxide, and PC concentrations increasing by 46.42%, 36.73%, and 52.00%, respectively, compared to the control group. Additionally, DN animals showed marked reductions in the activity of antioxidant enzymes; SOD, CAT, GST, and GPx were decreased by 50.00%, 57.86%, 52.55%, and 40.23%, respectively ($p = 0.001$), relative to the control group (Fig. 1 and Table 3).

Administration of EESP significantly mitigated these adverse effects. Group IV animals exhibited reduced levels of LPO, hydrogen peroxide, and PC, with reductions of 31.25%, 36.11%, and 38.88%, respectively, compared with the DN group. Additionally, there was an increase in the activity of SOD, CAT, GST, and GPx, with increases of 66.00%, 95.13%, 76.92%, and 47.86%, respectively, when compared to the untreated group III ($p = 0.001$).

The group receiving MET treatment (group V) exhibited significantly reduced levels of LPO, hydrogen peroxide, and PC, with reductions of 35.48%, 28.94%, and 51.51%, respectively, compared with the DN group. Additionally, there was an increase in the activities of SOD, CAT, GST, and GPx by 60.00%, 50.21%, 60.00%, and 44.26%, respectively, relative to those in the DN group ($p = 0.001$). The results suggest that the administration of EESP and MET effectively reduced oxidative stress and enhanced antioxidant defense mechanisms in the renal tissue of rats with DN, with EESP demonstrating a superior effect compared to MET.

3.4. Histopathological changes

3.4.1. Hematoxylin and eosin

Upon microscopic examination, the kidney sections of both the control group and the group administered EESP demonstrated normal renal architecture (Fig. 2A1 and A2). In contrast, the untreated DN group exhibited degeneration and necrosis of the renal parenchymal cells along with thickening of the GBM (Fig. 2A3). However, the diabetes-induced group that received EESP treatment showed a normative glomerulus with minimal tubular necrosis and congestion within the glomerulus, indicating recovery from nephropathic changes (Fig. 2A4). Animals with DN treated with MET displayed normal glomeruli with Bowman's capsule and dilated renal tubules, with minimal signs of

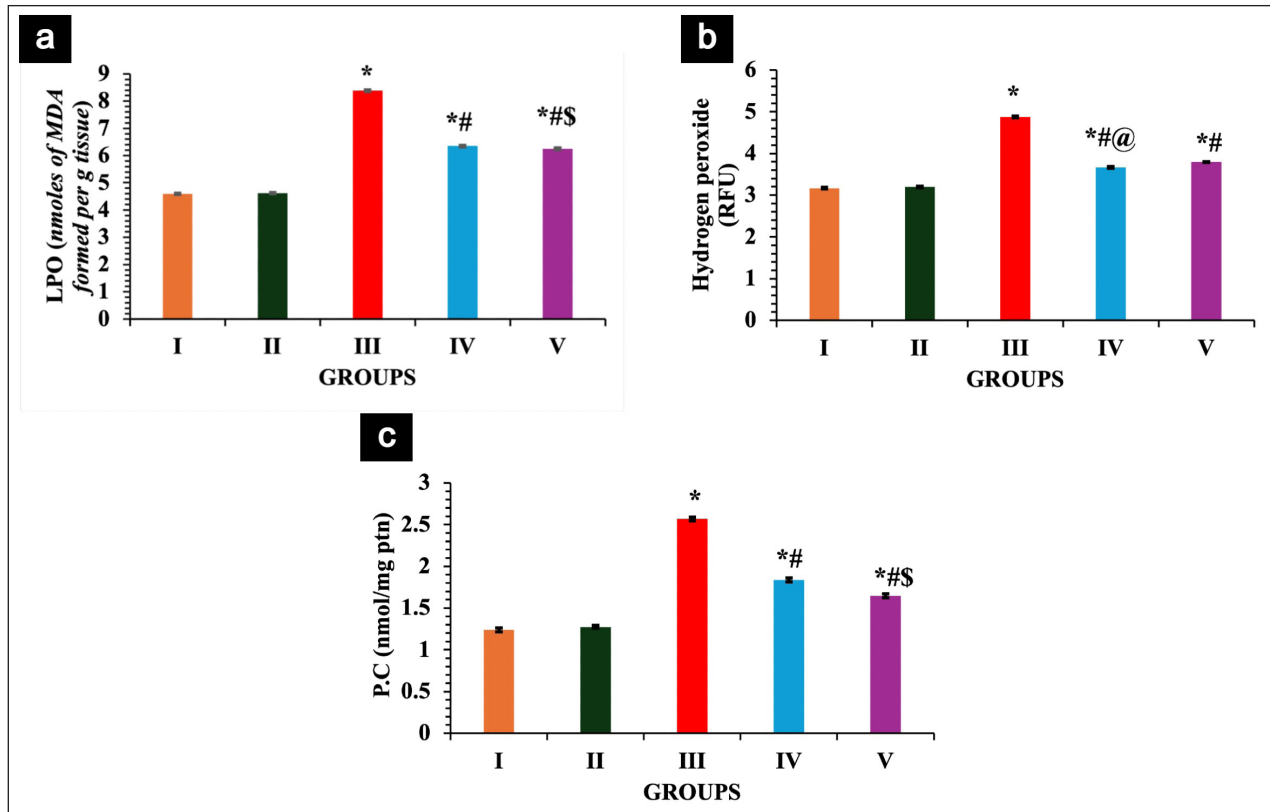


Figure 1. Graph showing oxidative stress markers in kidney tissue. Results are expressed as the mean \pm SD ($n = 6$). The superscripts indicate a significant difference between groups based on the Tukey post hoc test following one-way ANOVA ($p \leq 0.05$). *: Compared with group I; #: Compared with group III; S: Compared with group IV; @: Compared with group V.

Table 3. Antioxidant enzymes levels in kidney tissue.

Group	SOD (U/mg protein)	CAT (nmoles of H ₂ O ₂ decomposed / min/mg protein)	GPX (nmoles of GSH utilized/ sec/mg protein)	GST (μ mol CDNB conjugate formed/min/mg protein)
I	6.43 \pm 0.01	4.58 \pm 0.01	32.51 \pm 0.28	1.73 \pm 0.01
II	6.46 \pm 0.02	4.56 \pm 0.01	32.41 \pm 0.31	1.34 \pm 0.02
III	2.94 \pm 0.02*	1.93 \pm 0.02*	19.43 \pm 0.16*	0.65 \pm 0.02*
IV	4.99 \pm 0.02*#@	3.38 \pm 0.02*#@	28.73 \pm 0.13*#@	1.15 \pm 0.02*#@
V	4.64 \pm 0.02*#	3.15 \pm 0.02*#	28.03 \pm 0.41*#	1.04 \pm 0.03*#

Results are expressed as the mean \pm SD ($n = 6$). The superscripts indicate a significant difference between groups based on the Tukey post hoc test following one-way ANOVA ($p \leq 0.05$). *: Compared with group I; #: Compared with group III; @: Compared with group V.

tubular necrosis and glomerular congestion (Fig. 2A5). When compared to the control group, a significant increase in the diameters of the glomerulus ($U = 370.50$, $p = 0.001$) and tubules ($U = 77.00$, $p = 0.001$) was observed in the renal tissues of group III animals (Fig. 3a and b), indicating a disruption in the structural integrity of these components due to STZ. These pathological changes were mitigated by

the administration of EESP, as demonstrated by a notable reduction in the diameters of the glomerulus ($U = 1147.50$, $p = 0.001$) and tubules ($U = 612.50$, $p = 0.002$) compared to those in untreated animals, approaching the levels observed in the control groups. A comparable trend of reduction in glomerular ($U = 774.50$, $p = 0.001$) and tubular ($U = 165.00$, $p = 0.001$) diameters was observed in MET-treated diabetic rats. When comparing the effects of EESP and MET on glomerular and tubular diameters, MET demonstrated a significantly greater impact ($p = 0.04$). In conclusion, both EESP and MET mitigated renal damage in DN, which is attributable to their nephroprotective properties.

3.4.2. Periodic acid-Schiff

PAS staining revealed that groups I and II normal GBM and mesangial areas located at the periphery of the renal cortex (Fig. 2B1 and B2). In the untreated DN group, there was discernible thickening of the GBM accompanied by expansion of the mesangial area, which was associated with cortical tubular necrosis (Fig. 2B3). Conversely, diabetic animals treated with EESP demonstrated a reduced expansion of the mesangial area and thickening of the GBM (Fig. 2B4). Animals in Group V, treated with MET, exhibited a progressive trend similar to that observed with EESP treatment (Fig. 2B5).

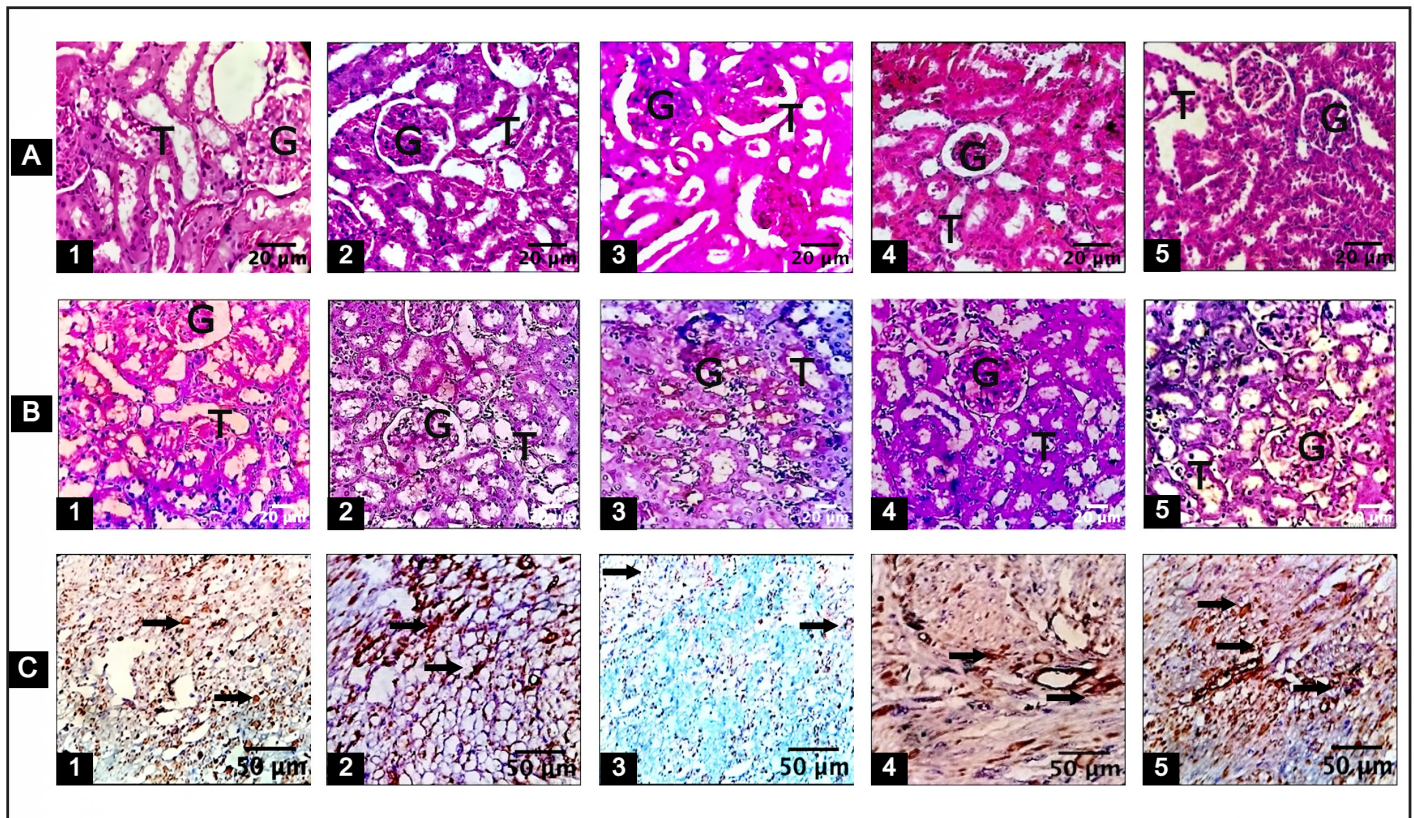


Figure 2. Histopathological and immunohistochemical changes in the renal tissue. A: H&E, B: PAS, Scale bar = 20 μm , 400 \times magnification, and C: ZO-1IHC Scale bar = 50 μm , magnification 100 \times ($n = 6$). G: Glomerulus, T: Tubules, Black arrow: ZO-1 positive cells.

3.4.3. Immunohistochemistry

Control animals, and those administered EESP, showed typical ZO-1 expression (Fig. 2C1, 2C2). In contrast, semi-quantitative assessment of ZO-1 immunopositivity of Group III, comprising untreated DN rats, indicated approximately threefold lower staining intensity compared to control rats (Fig. 2C4 and 3C). The diabetic rats administered EESP and MET demonstrated a 2.5- and 2.85-fold higher staining intensity, respectively, compared to the untreated DN group, indicating the potential role of these experimental drugs in modulating ZO-1 expression (Fig. 2C4, C5, and 3C).

3.5. Ultrastructural changes

EM analysis of renal tissues from the control group revealed well-preserved architectural integrity, with podocytes exhibiting intact foot processes, glomeruli, mesangial cells with prominent nuclei, and mitochondria displaying cristae (Fig. 4). In contrast, untreated DN animals exhibited aberrant glomeruli surrounded by vacuoles (Fig. 4A3), reduced podocyte nuclei, effaced foot processes, and diminished distal convoluted tubules (DCT) (Fig. 4D3). The mitochondria lacking cristae (Fig. 4E3), shrunken mesangial cells, and thickened tubular basement membrane (Fig. 4F3) were also observed in DN rats. Group IV demonstrated notable preservation of the renal architecture. Podocytes showed less pronounced basement membrane thickening and reduced foot process effacement (Fig. 4B4). Proximal tubules appeared more intact (Fig. 4C4),

with a better-preserved mitochondrial structure (Fig. 4D4). Group (5) exhibited protective effects, with glomeruli showing reduced foot process effacement (Fig. 4B5), and proximal tubules appeared healthier than those in the DN and IV groups. These ultrastructural findings support urine analysis, indicating that STZ-induced diabetes caused significant kidney damage, whereas treatment with both EESP and MET mitigated these pathological changes.

3.6. *Tjp1* gene expression

Rats in group III demonstrated a 3.5-fold decrease in *Tjp1* expression ($p = 0.02$). Conversely, the mRNA levels of *Tjp1* were considerably elevated in the diabetic groups administered with EESP and MET (groups IV and V), leading to a substantial increase in *Tjp1* gene expression (2.25-fold, $p = 0.03$ and 2.9-fold, $p = 0.01$, respectively) compared to group III. In group II, the administration of EESP did not cause any significant variation in the levels of *Tjp1* expression when compared to the control group. Group V animals treated with MET demonstrated higher *Tjp1* expression than the EESP-treated group ($p = 0.03$) (Fig. 5a and b).

3.7. ZO-1 immuno blot

Western blot analysis of ZO-1 protein revealed significant differences among the various experimental groups, as illustrated in Figure 6. The expression of this protein was reduced by 4.8-fold in group III compared to that

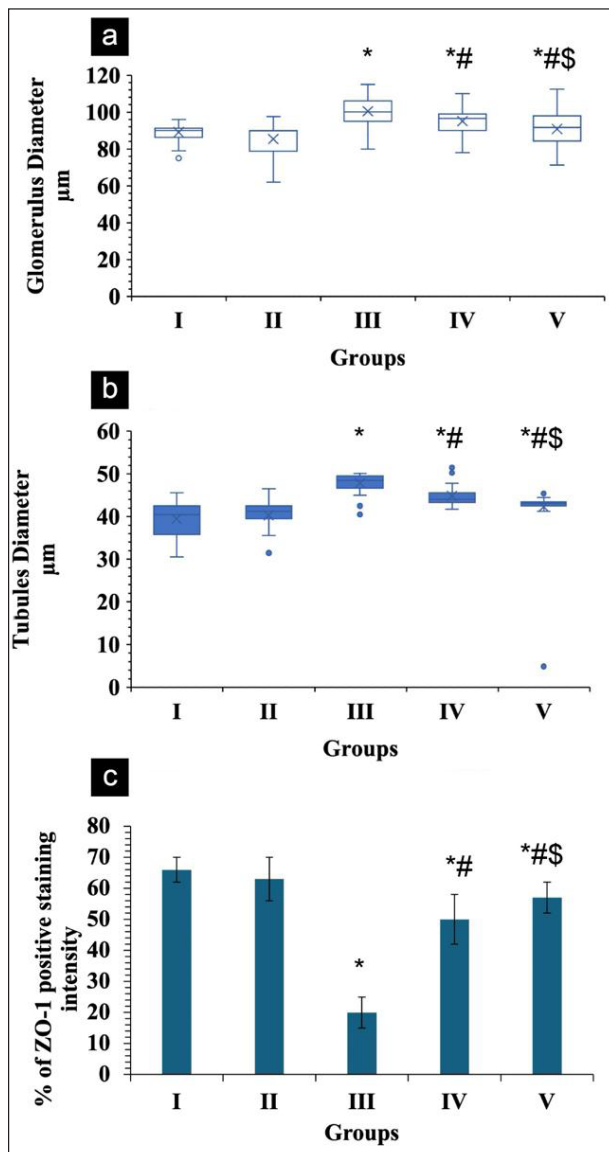


Figure 3. Morphometric analysis of glomerulus and tubules diameter and the staining intensity of ZO-1 expression in various groups. Box-and-whisker plot showing (a) glomerular diameter and (b) shows the tubular diameter across experimental groups. Data represent median with interquartile range; whiskers indicate minimum and maximum values, and outliers are shown as individual points. The superscripts indicate a significant difference between the groups based on Dunn's test with Bonferroni correction following the Kruskal-Wallis test ($p \leq 0.05$). (c) shows the semi-quantitative assessment of staining intensity of ZO-1 expression in the various groups. Superscripts indicate significant differences between groups based on Tukey's post-hoc test following one-way ANOVA ($p \leq 0.05$). *: Compared with Group I; #: Compared with Group III; \$: Compared with Group IV.

in group I ($p = 0.001$). Animals in groups IV and V exhibited significantly increased levels of ZO-1 protein expression relative to that in group III, with increases of 3.6-fold ($p = 0.01$) and 3.8-fold ($p = 0.002$), respectively. It is important to note that ZO-1 expression levels were markedly elevated in normal rats as well as in those treated exclusively with EESP (Fig. 6a and b).

4. DISCUSSION

The present study demonstrated that EESP exerted renoprotective effects in STZ-induced DN by reducing oxidative stress, restoring renal function, improving renal histoarchitecture, and modulating the expression of the TJ protein ZO-1. These findings suggested that EESP may serve as a promising complementary therapeutic agent for DN by targeting multiple pathological pathways.

4.1. Amelioration of diabetic symptoms and metabolic dysregulation

Administration of EESP effectively mitigated hallmark diabetic symptoms, including polyphagia and polydipsia, while improving glycemic control. In a previous study, we documented the hypoglycemic properties of EESP, highlighting its potential to enhance fasting insulin levels and its role in the expression of FSP-1 in modulating EMT and ameliorating renal fibrosis [19]. Notably, similar effects were observed in alloxan-induced diabetic models, where EESP (100 mg/kg) improved the glycemic status without significantly altering insulin levels, suggesting an extrapancreatic mechanism of action [20]. Our findings corroborate previous reports on the hypoglycemic properties of EESP, thereby restoring metabolic homeostasis. However, further investigation is required to elucidate whether EESP enhances insulin sensitivity or stimulates residual beta-cell function.

4.2. Restoration of renal function and biochemical parameters

DN is characterized by progressive renal dysfunction, as evidenced by elevated urinary urea and creatinine levels and proteinuria. In this study, EESP administration significantly improved these parameters, indicating a preserved renal filtration capacity. These findings align with past research showing the nephroprotective effects of EESP against gentamycin-induced nephrotoxicity [21]. Bioactive phytochemicals such as berberine, resveratrol, and puerarin have been shown to reduce proteinuria and normalize renal biomarkers through antioxidative and anti-inflammatory mechanisms [31]. Given the established antioxidant properties of EESP, it is plausible that similar pathways contribute to its therapeutic efficacy in DN.

4.3. Attenuation of oxidative stress and enhancement of endogenous antioxidant defenses

Hyperglycemia-induced oxidative stress is a key driver of DN progression, primarily through nicotinamide adenine dinucleotide phosphate oxidase- and nitric oxide synthase-dependent pathways in glomeruli and proximal tubules [32]. Elevated intracellular glucose levels promote the overproduction of reactive oxygen species (ROS), leading to LPO, PC formation, and DNA damage. In this study, EESP significantly reduced the levels of oxidative stress markers (LPO, hydrogen peroxide, and PC) and enhanced the activity of antioxidant enzymes (SOD, CAT, GPx, and GST) in renal tissues of diabetic animals. The present findings align with prior research that has demonstrated the antioxidative properties of EESP in models of type 2 diabetes [33].

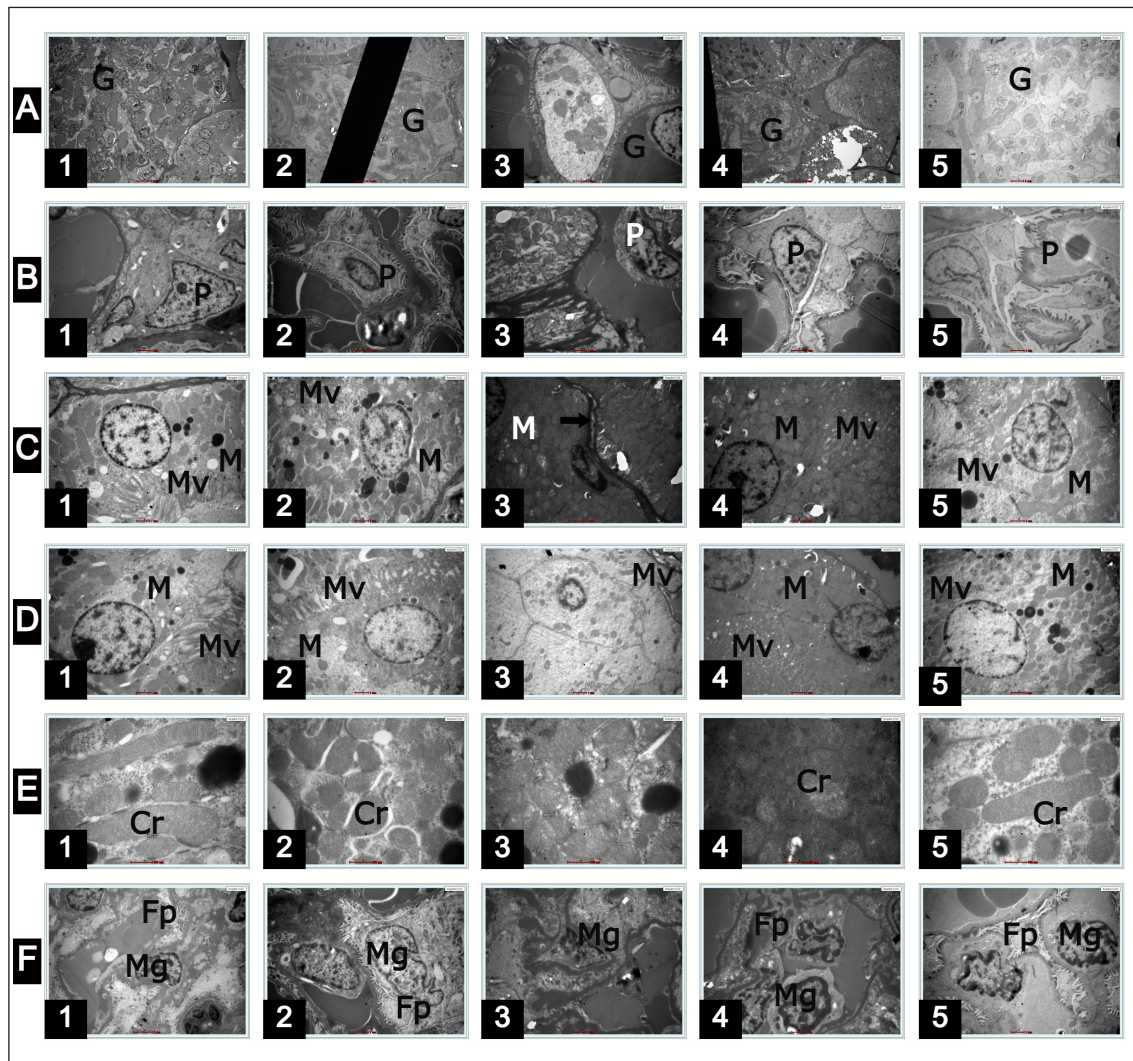


Figure 4. Electron micrographs of renal tissues of the different groups. (A): Glomerulus (1,050 \times magnification), (B): Podocytes with foot process (6,000 \times magnification), (C): Proximal convoluted tubule (PCT) (6,000 \times magnification), (D): DCT (6,000 \times magnification), (E): Mitochondria (20,000 \times magnification), and (F): Mesangial cells (6,000 \times magnification). Numbers 1–5 indicate experimental groups. G: Glomerulus, P: Podocyte, M: Mitochondria, Mv: Microvilli, Mg: Mesangial cells, Fp: Foot process, Cr: Cristae, Black arrow: Thickening of the basement membrane.

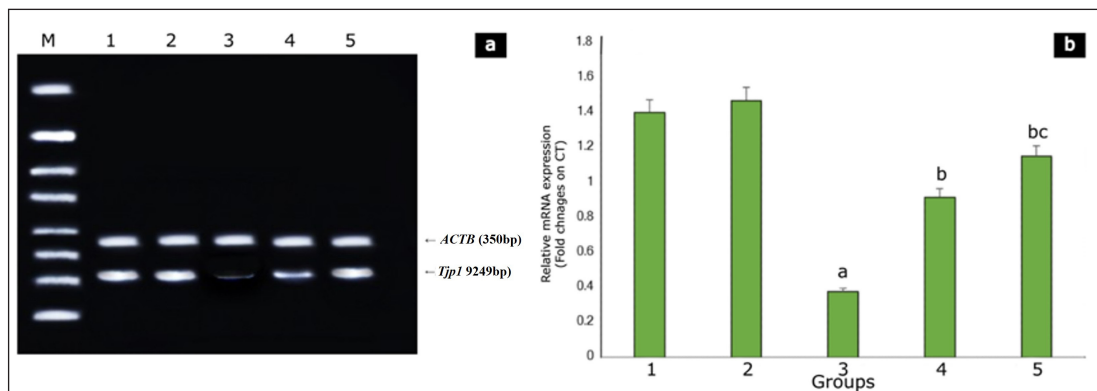


Figure 5. mRNA expression of *Tjp1* gene in rat kidney. (a) shows a representative gel image of *Tjp1* expression in the various groups. M: Marker Lane (100–1,000 Bp). Numbers 1–5 indicate experimental groups. (b) shows the relative *Tjp1* expression levels in different groups. Values are represented as the mean \pm SD ($n = 6$). Superscripts indicate significant differences between groups based on Tukey's post-hoc test following one-way ANOVA ($p \leq 0.05$). a: Comparison with group I; b: Comparison with group III; c: Comparison with group IV.

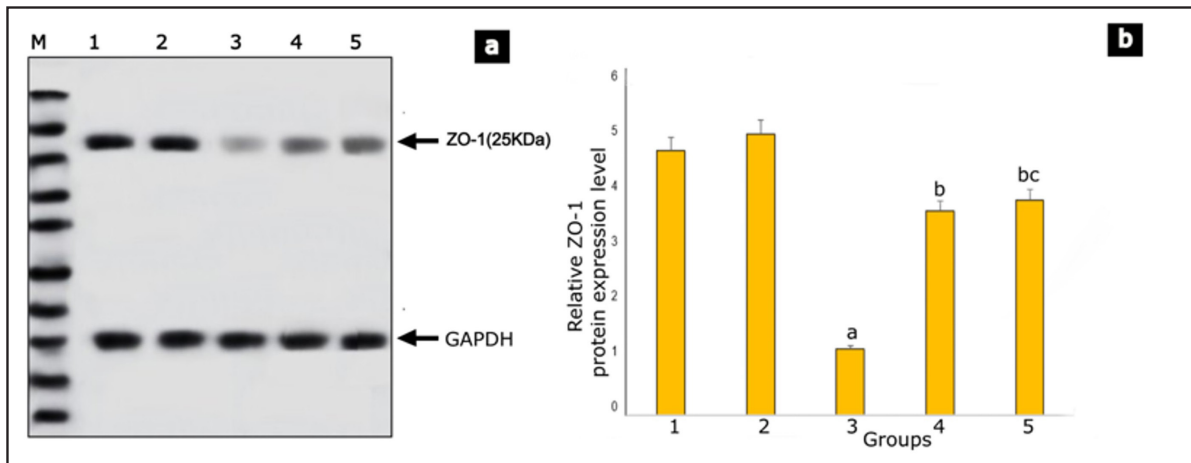


Figure 6. ZO-1 Protein expression in rat kidney. (a) shows a representative gel image of ZO-1 protein expression in the various groups. Lane M- Marker Lane (10–100 kDa). Numbers 1–5 indicate experimental groups. (b) shows the relative ZO-1 protein expression levels in different groups. Values are represented as the mean \pm SD ($n = 6$). Superscripts indicate significant differences between groups based on Tukey's *post-hoc* test following one-way ANOVA ($p \leq 0.05$). a: Comparison with group I; b: Comparison with group III; c: Comparison with group IV.

The antioxidative properties of EESP are comparable to those of well-characterized phytochemicals, such as curcumin and resveratrol, which mitigate renal damage by scavenging ROS and upregulating endogenous antioxidant defenses [34,35]. Given the central role of free radical damage in DN pathogenesis, the ability of EESP to reestablish redox equilibrium may underlie its renoprotective effects.

4.4. Structural preservation of renal architecture

Histopathological and EM analyses revealed that EESP administration attenuated GBM thickening, tubular atrophy, and interstitial fibrosis, which are the hallmark features of DN. PAS staining confirmed a reduction in GBM thickening, suggesting that EESP preserved the integrity of the glomerular filtration barrier. The results align with earlier studies regarding EESP's capacity to mitigate tubular necrosis and inflammatory cell infiltration in gentamycin-induced nephrotoxicity [21].

The structural improvements observed in this study could be linked to the antioxidative and anti-inflammatory properties of EESP, which prevent extracellular matrix accumulation and fibrosis. Similar effects have been reported for thymoquinone (from *Nigella sativa*), which enhances ZO-1 expression and ameliorates histopathological damage in STZ-induced DN [36].

4.5. Modulation of ZO-1 expression and podocyte integrity

TJ proteins, particularly ZO-1, play critical roles in maintaining podocyte SD integrity and in preventing proteinuria. Under diabetic conditions, oxidative stress disrupts ZO-1 localization, leading to cytosolic delocalization, claudin polymerization, and SD dysfunction [32,37]. Our study demonstrated that EESP upregulates ZO-1 expression at both the transcriptional and translational levels, suggesting a direct role in preserving podocyte structure and function.

Bioactive phytochemicals, including 2,3,5,4'-Tetrahydroxystilbene-2-O- β -D-glucoside, piperazine ferulate, and chrysin, as well as pharmacological agents such

as simvastatin, sirolimus, and AM251, along with traditional medicines such as the Huajuxiaoji formula and Kunxian capsule, have been demonstrated to enhance ZO-1 expression through distinct mechanisms.

2,3,5,4'-Tetrahydroxystilbene-2-O- β -D-glucoside, derived from *Polygonum multiflorum*, restores ZO-1 expression by targeting the renin-angiotensin system, thereby reducing renal fibrosis [38]. Additionally, EESP may share mechanisms with piperazine ferulate (which activates AMP-activated protein kinase (AMPK) to protect the endothelial glycocalyx) and chrysin (which restores ZO-1/occludin expression to prevent EMT) [39,40]. The effects of EESP align with those of these agents, particularly their ability to counteract oxidative stress-induced ZO-1 degradation.

Simvastatin, a statin with pleiotropic effects, enhances ZO-1 expression by inhibiting the Ras homolog family member A/Rho-associated kinase 1 (RhoA/ROCK1) pathway, thereby preserving podocyte integrity [41]. Sirolimus, a mammalian target of Rapamycin (mTOR) inhibitor, upregulates ZO-1 in early stage DN (8 weeks), but fails to sustain its expression in advanced stages (20 weeks), leading to proteinuria [42]. This underscores the need for long-term studies on the efficacy of EESP. AM251, a cannabinoid receptor 1 antagonist, reduces albuminuria by upregulating ZO-1 and counteracting podocyte cannabinoid receptor overexpression in diabetes [43].

Huajuxiaoji and Kunxian capsules have been demonstrated to upregulate ZO-1 by inhibiting the NOD-, LRR-, and pyrin domain-containing protein 3 inflammasome and suppressing the wntless-related integration site (Wnt)/ β -catenin pathway, respectively [44,45]. Notably, the Kunxian capsule did not affect blood glucose levels, highlighting the additional advantage of EESP in glycemic control. While the above-mentioned bioactive phytochemicals are known to influence ZO-1 expression through pathways such as AMPK, RhoA/ROCK1, mTOR, and Wnt/ β -catenin, EESP exhibited comparable antioxidant activity and was associated with enhanced ZO-1 expression in the present study. Although

specific signaling pathways were not evaluated, the similarity in antioxidant properties suggests a possible association with these pathways, warranting further investigation.

Interestingly, conflicting reports have been published regarding ZO-1 expression in DN patients. While many studies have indicated ZO-1 downregulation due to oxidative stress, others have reported impaired autophagic flux, leading to ZO-1 accumulation and podocyte effacement [46]. These discrepancies may arise from differences in disease progression or in experimental models. Our findings support the former hypothesis, as the antioxidative effects of EESP likely prevent ZO-1 degradation and restore the normal expression patterns.

4.6. Broader implications for diabetic complications

In retinal endothelial cells, ZO-1 degradation exacerbates vascular permeability and inflammation [47]. Similarly, hyperglycemia-induced ZO-1 downregulation in airway epithelia increases susceptibility to infections [48]. Given the ability of EESP to enhance ZO-1 expression and mitigate oxidative stress, it may hold therapeutic potential for these complications, warranting further investigations. In this study, the MET treatment demonstrated superior efficacy on renal parameters compared to EESP. However, EESP exhibited a more pronounced antioxidant effect, which holds broader implications given the critical role of oxidative damage and inflammatory mechanisms in the development of DM and its complications.

4.7. Future directions and clinical implications

Although our findings highlight renoprotective potential of EESP, several questions remain unanswered. First, the specific molecular pathways (e.g., AMPK, RhoA/ROCK1, mTOR, and Wnt/ β -catenin) through which EESP can possibly modulate ZO-1 require further elucidation. Second, it is imperative to conduct long-term clinical trials to evaluate whether EESP maintains its efficacy in advanced DN, similar to the observations with sirolimus, which has been found ineffective in late-stage diseases [40], as well as to assess its safety.

4.8. Limitations

The limitations of this research include its brief duration (30 days) and the lack of a direct evaluation of inflammatory mediators, which may have offered deeper insights into the mechanisms by which EESP operates. Additionally, an exploration of the specific cellular pathways implicated in the documented effects would significantly enrich our understanding of EESP's nephroprotective properties. Moreover, the difficulties associated with extrapolating these findings from animal models to human populations, potential adverse effects stemming from prolonged use, and interactions with other pharmaceutical agents have not been examined.

5. CONCLUSION

In summary, EESP demonstrated significant renoprotective effects in STZ-induced DN. It effectively improved renal function, mitigated oxidative stress, and preserved the renal histoarchitecture. Notably, EESP enhanced

the expression of the tight junction protein ZO-1, suggesting its role in maintaining the integrity of the glomerular filtration barrier. These multifaceted effects highlight EESP as a potential therapeutic candidate for DN. Future research focusing on the specific molecular pathways by which EESP exerts its effects is needed, along with long-term studies and clinical trials to validate its safety and efficacy in advanced stages of DN.

6. LIST OF ABBREVIATIONS

ACTB, Actin beta; AMPK, AMP-Activated Protein Kinase; CAT, Catalase; DCT, Distal convoluted tubule; DM, Diabetes mellitus DN, Diabetic nephropathy; EESP, Ethanolic extract of *Strychnos potatorum*; EM, Electron microscopic; EMT, Epithelial mesenchymal transition; ESRD, End stage renal disease; FSP-1, Fibroblast-specific protein 1; GAPDH, Glyceraldehyde-3-phosphate dehydrogenase; GBM, Glomerular basement membrane; GFR, Glomerular filtration rate; GPx, Glutathione peroxidase; GST, Glutathione-S-transferase; H&E, Hematoxylin and eosin; IHC, Immunohistochemistry; LPO, Lipid peroxide; MET, Metformin; mTOR, Mammalian target of Rapamycin; PAS, Periodic Acid-Schiff Stain; PC, Protein carbonyls; PCT, Proximal convoluted tubule; RhoA/ROCK1, Ras homolog family member A / Rho-associated kinase 1; ROS, Reactive oxygen species; SD, Slit Diaphragms; SOD, Superoxide dismutase; STZ, Streptozotocin; *Tjp1*, Tight junction protein 1; TJ, Tight junctions; Wnt, Wingless-related integration site; ZO-1, Zonula occludens – 1.

7. AUTHOR CONTRIBUTIONS

All authors made substantial contributions to conception and design, acquisition of data, or analysis and interpretation of data; took part in drafting the article or revising it critically for important intellectual content; agreed to submit to the current journal; gave final approval of the version to be published; and agree to be accountable for all aspects of the work. All the authors are eligible to be author as per the International Committee of Medical Journal Editors (ICMJE) requirements/guidelines.

8. FINANCIAL SUPPORT

This work received no specific grants from any funding agency in public, commercial, or nonprofit organizations.

9. CONFLICTS OF INTEREST

The authors report no financial or any other conflicts of interest in this work.

10. ETHICAL APPROVALS

The experimental protocol was approved by the Institutional Animal Ethics Committee of the Chettinad Hospital and Research Institute (IAEC 1/ Proposal:105/A. Lr: 78, Dt: 13.02.2023). This study was performed in accordance with the principles of the Committee for the Purpose of Control and Supervision of Experiments on Animals.

11. DATA AVAILABILITY

Data supporting the findings of this study are available from the corresponding author upon reasonable request.

12. PUBLISHER'S NOTE

All claims expressed in this article are solely those of the authors and do not necessarily represent those of the publisher, the editors and the reviewers. This journal remains neutral with regard to jurisdictional claims in published institutional affiliation.

13. USE OF ARTIFICIAL INTELLIGENCE (AI)-ASSISTED TECHNOLOGY

The authors declare that they have not used artificial intelligence (AI)-tools for writing and editing of the manuscript, and no images were manipulated using AI.

REFERENCES

- Zharkikh E, Dremin V, Zhrebtsov E, Dunaev A, Meglinski I. Biophotonics methods for functional monitoring of complications of diabetes mellitus. *J Biophotonics*. 2020;13(10):e202000203. doi: <https://doi.org/10.1002/jbio.202000203>
- Alicic RZ, Rooney MT, Tuttle KR. Diabetic kidney disease: challenges, progress, and possibilities. *Clin J Am Soc Nephrol*. 2017;12(12):2032–45. doi: <https://doi.org/10.2215/CJN.11491116>
- Ma X, Liu R, Xi X, Zhuo H, Gu Y. Global burden of chronic kidney disease due to diabetes mellitus, 1990-2021, and projections to 2050. *Front Endocrinol (Lausanne)*. 2025;16:1513008. doi: <https://doi.org/10.3389/fendo.2025.1513008>
- Viswanathan V, Mirshad R. The burden of DN in India: need for prevention. *Diabet Nephrop*. 2023;3(2):25–8. doi: <https://doi.org/10.2478/dine-2023-0003>
- Dagar N, Das P, Bisht P, Taraphdar AK, Velayutham R, Arumugam S. Diabetic nephropathy: a twisted thread to unravel. *Life Sci*. 2021;278:119635. doi: <https://doi.org/10.1016/j.lfs.2021.119635>
- Hahr AJ, Molitch ME. Management of diabetes mellitus in patients with chronic kidney disease. *Clin Diabetes Endocrinol*. 2015;1:2. doi: <https://doi.org/10.1186/s40842-015-0001-9>
- Perico L, Conti S, Benigni A, Remuzzi G. Podocyte-actin dynamics in health and disease. *Nat Rev Nephrol*. 2016;12(11):692–710. doi: <https://doi.org/10.1038/nrneph.2016.127>
- Lee DB, Huang E, Ward HJ. Tight junction biology and kidney dysfunction. *Am J Physiol Renal Physiol*. 2006;290(1):F20–34. doi: <https://doi.org/10.1152/ajprenal.00052.2005>
- Fukasawa H, Bornheimer S, Kudlicka K, Farquhar MG. Slit diaphragms contain tight junction proteins. *J Am Soc Nephrol*. 2009;20(7):1491–503. doi: <https://doi.org/10.1681/ASN.2008101117>
- Kurihara H, Anderson JM, Kerjaschki D, Farquhar MG. The altered glomerular filtration slits seen in puromycin aminonucleoside nephrosis and protamine sulfate-treated rats contain the tight junction protein ZO-1. *Am J Pathol*. 1992;141(4):805–16.
- Morita Y, Hida M, Takahashi A, Nihei H, Kashiwagi T. Inducible expression of claudin-1 in glomerular podocytes generates aberrant tight junctions and proteinuria through slit diaphragm destabilization. *J Am Soc Nephrol*. 2017;28(1):106–17. doi: <https://doi.org/10.1681/ASN.2015121324>
- Hasegawa K, Wakino S, Simic P, Sakamaki Y, Minakuchi H, Fujimura K, *et al*. Renal tubular Sirt1 attenuates diabetic albuminuria by epigenetically suppressing claudin-1 overexpression in podocytes. *Nat Med*. 2013;19(11):1496–504. doi: <https://doi.org/10.1038/nm.3363>
- Ying Q, Wu G. Molecular mechanisms involved in podocyte EMT and concomitant diabetic kidney diseases: an update. *Ren Fail*. 2017;39(1):474–83. doi: <https://doi.org/10.1080/0886022X.2017.1313164>
- Tomino Y, Gohda T. The prevalence and management of diabetic nephropathy in Asia. *Kidney Dis (Basel)*. 2015;1(1):52–60. doi: <https://doi.org/10.1159/000381757>
- Samsu N. Diabetic nephropathy: challenges in pathogenesis, diagnosis, and treatment. *Biomed Res Int*. 2021;2021:1497449. doi: <https://doi.org/10.1155/2021/1497449>
- Yadav K, Kadam P, Patel J, Patil M. *Strychnos potatorum*: phytochemical and pharmacological review. *Pharmacogn Rev*. 2014;8(15):61–6. doi: <https://doi.org/10.4103/0973-7847.125533>
- Shankaranarayanan A, Subramanian M, Periyasamy R, Anbumani SK, Raj Thomson JE, Venugopal N. Phytochemical screening, HPTLC, GC-MS and in vitro antioxidant analyses of ethanol extract of *Strychnos potatorum* seeds. *J Nat Remedies*. 2025;25(6):1335–46. doi: <https://doi.org/10.18311/jnr/2025/47431>
- Sanmugapriya E, Venkataraman S. Toxicological investigations on *Strychnos potatorum* Linn seeds in experimental animal models. *J Health Sci*. 2006;52:339–43. doi: <https://doi.org/10.1248/jhs.52.339>
- Shankaranarayanan A, Subramanian M, Raj Thomson JE, Anbumani SK. Protective effects of *Strychnos potatorum* seed extract on diabetic nephropathy in rats: downregulation of FSP-1 expression. *J Appl Pharm Sci*. 2025;15(07):193–202. doi: <https://doi.org/10.7324/JAPS.2025.233971>
- Dhasarathan P, Theriappan P. Evaluation of antidiabetic activity of *Strychnos potatorum* in alloxan-induced diabetic rats. *J Med Med Sci*. 2011;2(2):670–4.
- Varghese R, Moideen MM, Suhail MJM, Dhanapal CK. Nephroprotective effect of ethanolic extract of *Strychnos potatorum* seeds in rat models. *Res J Pharm Biol Chem Sci*. 2011;2(3):521–9.
- Punithavathi VR, Prince PSM, Kumar R, Selvakumari J. Antihyperglycaemic, antilipid peroxidative and antioxidant effects of gallic acid on streptozotocin-induced diabetic Wistar rats. *Eur J Pharmacol*. 2011;650(1):465–71. doi: <https://doi.org/10.1016/j.ejphar.2010.08.059>
- Jittiwat J, Chonpathompikunlert P, Sukketsiri W. Neuroprotective effects of *Apium graveolens* against focal cerebral ischemia occur partly via antioxidant, anti-inflammatory, and anti-apoptotic pathways. *J Sci Food Agric*. 2021;101(6):2256–63. doi: <https://doi.org/10.1002/jsfa.10846>
- Farhat F, Simon B, Amérand A, Devaux J, Belhomme M, Calves P, *et al*. Exercise training changes mitochondrial function and its vulnerability to reactive oxygen species exposure differently in male and female silver European eels. *Environ Biol Fish*. 2020;103(4):363–75. doi: <https://doi.org/10.1007/s10641-020-00962-z>
- Varadacharyulu N, Swarnalatha K, Fareeda Begum S, Mohan Chandra M, Ramaiah CV. Alcohol exacerbated nitroxidative stress in brain of diabetic rats: an ameliorative role of green tea. *Indian J Neurosci*. 2021;7:106–18. doi: <https://doi.org/10.18231/j.ijn.2021.018>
- Atamanalp M, Alak G, Fakoğlu O, Uçar A, Parlak V. The effects of biopesticide on the antioxidant enzyme activities of Lemna minor. *OFOAJ*. 2019;9(3):1–5. doi: <https://doi.org/10.19080/OFOAJ.2019.09.555761>
- Zahouani Y, Ben Rhouma K, Kacem K, Sebai H, Sakly M. Aqueous leaf extract of *Pistacia lentiscus* improves acute acetic acid-induced colitis in rats by reducing inflammation and oxidative stress. *J Med Food*. 2021;24(7):697–708. doi: <https://doi.org/10.1089/jmf.2020.0020>
- Payamalle S, Joseph KS, Bijjaragi SC, Aware C, Jadhav JP, Murthy HN. Antidiabetic activity of *Garcinia xanthochymus* seeds. *Comp Clin Pathol*. 2017;26(2):437–46. doi: <https://doi.org/10.1007/s00580-016-2396-9>
- Subramanian M, Thotakura B, Chandra Sekaran SP, Jyothi AK, Sundaramurthi I. Naringin ameliorates streptozotocin-induced diabetes through FOXM1-mediated β cell proliferation. *Cells Tissues Organs*. 2018;206(4-5):242–53. doi: <https://doi.org/10.1159/000499480>
- Subramanian M, Thotakura B, Chandra Sekaran SP, Jyothi AK, Sundaramurthi I. Naringin (4',5,7-trihydroxyflavone 7-rhamnoglucoside) attenuates β -cell dysfunction in diabetic

- rats through upregulation of PDX-1. *Cells Tissues Organs*. 2018;206(3):133–43. doi: <https://doi.org/10.1159/000496506>
31. Hu S, Wang J, Liu E, Zhang X, Xiang J, Li W, *et al.* Protective effect of berberine in diabetic nephropathy: a systematic review and meta-analysis revealing the mechanism of action. *Pharmacol Res*. 2022;185:106481. doi: <https://doi.org/10.1016/j.phrs.2022.106481>
 32. Molina-Jijón E, Rodríguez-Muñoz R, Namorado MDC, Pedraza-Chaverri J, Reyes JL. Oxidative stress induces claudin-2 nitration in experimental type 1 diabetic nephropathy. *Free Radic Biol Med*. 2014;72:162–75. doi: <https://doi.org/10.1016/j.freeradbiomed.2014.03.040>
 33. Subramanian SP. Evaluation of antidiabetic and antioxidative efficacy of *Strychnos potatorum* (Nirmali) seeds extract in high fat diet fed–low dose streptozotocin induced experimental type 2 diabetes in rats. *Diabetes*. 2020;6(1):1–8. doi: <https://doi.org/10.15562/diabetes.2020.63>
 34. Kitada M, Koya D. Renal protective effects of resveratrol. *Oxid Med Cell Longev*. 2013;2013:568093. doi: <https://doi.org/10.1155/2013/568093>
 35. Trujillo J, Chirino YI, Molina-Jijón E, Andérica-Romero AC, Tapia E, Pedraza-Chaverri J. Renoprotective effect of the antioxidant curcumin: recent findings. *Redox Biol*. 2013;1(1):448–56. doi: <https://doi.org/10.1016/j.redox.2013.09.003>
 36. Omran OM. Effects of thymoquinone on STZ-induced diabetic nephropathy: an immunohistochemical study. *Ultrastruct Pathol*. 2014;38(1):26–33. doi: <https://doi.org/10.3109/01913123.2013.830166>
 37. Eftekhari A, Vahed SZ, Kavetsky T, Rameshrad M, Jafari S, Chodari L, *et al.* Cell junction proteins: crossing the glomerular filtration barrier in diabetic nephropathy. *Int J Biol Macromol*. 2020;148:475–82. doi: <https://doi.org/10.1016/j.ijbiomac.2020.01.168>
 38. Chen GT, Yang M, Chen BB, Song Y, Zhang W, Zhang Y. 2,3,5,4'-Tetrahydroxystilbene-2-O-β-d-glucoside exerts protective effects on diabetic nephropathy in mice with hyperglycemia induced by streptozotocin. *Food Funct*. 2016;7(11):4628–36. doi: <https://doi.org/10.1039/c6fo01319h>
 39. Yang YY, Chen Z, Yang XD, Deng RR, Shi LX, Yao LY, *et al.* Piperazine ferulate prevents high-glucose-induced filtration barrier injury of glomerular endothelial cells. *Exp Ther Med*. 2021;22(4):1175. doi: <https://doi.org/10.3892/etm.2021.10607>
 40. Kang MK, Park SH, Choi YJ, Shin D, Kang YH. Chrysin inhibits diabetic renal tubulointerstitial fibrosis through blocking epithelial to mesenchymal transition. *J Mol Med (Berl)*. 2015;93(7):759–772. doi: <https://doi.org/10.1007/s00109-015-1301-3>
 41. Peng H, Luo P, Li Y, Wang C, Liu X, Ye Z, *et al.* Simvastatin alleviates hyperpermeability of glomerular endothelial cells in early-stage diabetic nephropathy by inhibition of RhoA/ROCK1. *PLoS One*. 2013;8(11):e80009. doi: <https://doi.org/10.1371/journal.pone.0080009>
 42. Wang J, Xu Z, Chen B, Zheng S, Xia P, Cai Y. The role of sirolimus in proteinuria in diabetic nephropathy rats. *Iran J Basic Med Sci*. 2017;20(12):1339–44. doi: <https://doi.org/10.22038/IJBMS.2017.9618>
 43. Gruden G, Barutta F, Kunos G, Pacher P. Role of the endocannabinoid system in diabetes and diabetic complications. *Br J Pharmacol*. 2016;173(7):1116–27. doi: <https://doi.org/10.1111/bph.13226>
 44. Zhang Z, Bi Y, Zhou F, Zhang D, Xu S, Zhang X, *et al.* Huajuxiaojia formula alleviates phenyl sulfate-induced diabetic kidney disease by inhibiting NLRP3 inflammasome activation and pyroptosis. *J Diabetes Res*. 2024;2024:8772009. doi: <https://doi.org/10.1155/2024/8772009>
 45. Jin B, Liu J, Zhu Y, Lu J, Zhang Q, Liang Y, *et al.* Kunxian capsule alleviates podocyte injury and proteinuria by inactivating β-catenin in db/db mice. *Front Med (Lausanne)*. 2023;10:1213191. doi: <https://doi.org/10.3389/fmed.2023.1213191>
 46. Wang B, Qian JY, Tang TT, Lin LL, Yu N, Guo HL, *et al.* VDR/Atg3 axis regulates slit diaphragm to tight junction transition via p62-mediated autophagy pathway in diabetic nephropathy. *Diabetes*. 2021;70(11):2639–51. doi: <https://doi.org/10.2337/db21-0205>
 47. Howell SJ, Lee CA, Batoki JC, Zapadka TE, Lindstrom SI, Taylor BE, *et al.* Retinal inflammation, oxidative stress, and vascular impairment is ablated in diabetic mice receiving XMD8-92 treatment. *Front Pharmacol*. 2021;12:732630. doi: <https://doi.org/10.3389/fphar.2021.732630>
 48. Yu H, Yang J, Zhou X, Xiao Q, Lü Y, Xia L. High glucose induces dysfunction of airway epithelial barrier through down-regulation of connexin 43. *Exp Cell Res*. 2016;342(1):11–9. doi: <https://doi.org/10.1016/j.yexcr.2016.02.012>

How to cite this article:

Shankaranarayanan A, Subramanian M, Aristotle S, Subramanian S, Kaliyaperumal P. Renoprotective effects of *Strychnos potatorum* seed extract in streptozotocin-induced diabetic nephropathy: Enhancement of antioxidant defenses and Zonula occludens – 1 expression. *J Appl Pharm Sci*. 2026;16(05):199-211. DOI: 10.7324/JAPS.2026.295760